TRPV1 acts as a synaptic protein and regulates vesicle recycling

Chandan Goswami[1,2,*,‡], Nils Rademacher[1], Karl-Heinz Smalla[3], Vera Kalscheuer[1], Hans-Hilger Ropers[1], Eckart D. Gundelfinger[3] and Tim Hucho[1]

[1]Signal Transduction in Pain and Mental Retardation, Department for Molecular Human Genetics, Max-Planck Institute for Molecular Genetics Ihnestrasse 73, 14195 Berlin, Germany
[2]School of Biological Sciences, National Institute of Science Education and Research (NISER), Institute of Physics Campus, Bhubaneswar, Orissa 751005, India
[3]Leibniz Institute for Neurobiology, Department of Neurochemistry/Molecular Biology, Brenneckestrasse 6, 39118 Magdeburg, Germany
*Author for correspondence (chandan@niser.ac.in)

Accepted 1 March 2010
Journal of Cell Science 123, 2045-2057

doi:10.1242/jcs.065144

Summary

Electrophysiological studies demonstrate that transient receptor potential vanilloid subtype 1 (TRPV1) is involved in neuronal transmission. Although it is expressed in the peripheral as well as the central nervous system, the questions remain whether TRPV1 is present in synaptic structures and whether it is involved in synaptic processes. In the present study we gathered evidence that TRPV1 can be detected in spines of cortical neurons, that it colocalizes with both pre- and postsynaptic proteins, and that it regulates spine morphology. Moreover, TRPV1 is also present in biochemically prepared synaptosomes endogenously. In F11 cells, a cell line derived from dorsal-root-ganglion neurons, TRPV1 is enriched in the tips of elongated filopodia and also at sites of cell-cell contact. In addition, we also detected TRPV1 in synaptic transport vesicles, and in transport packets within filopodia and neurites. Using FM4-64 dye, we demonstrate that recycling and/or fusion of these vesicles can be rapidly modulated by TRPV1 activation, leading to rapid reorganization of filopodial structure. These data suggest that TRPV1 is involved in processes such as neuronal network formation, synapse modulation and release of synaptic transmitters.

Key words: Capsaicin receptor, Synapse, Active zone, FM4-64 dye, Synaptic-vesicle recycling

Introduction

Transient receptor potential vanilloid subtype 1 (TRPV1), alternatively known as capsaicin receptor, is a member of the TRP superfamily (Caterina et al., 1997). It can be activated by different exogenous and endogenous ligands, and also by temperature (Caterina et al., 1997). Although previously known to be expressed exclusively in the dorsal root ganglion (DRG) neurons, later studies revealed a widespread expression of TRPV1 in brain, albeit at a much lower levels (Tóth et al., 2005; Roberts et al., 2004; Starowicz et al., 2008). Comparative immunohistochemical analyses of knockout and wild-type animals also confirmed that TRPV1 is present in the brain (Cristino et al., 2006). Endogenous expression of TRPV1 in different parts of the brain, in the spinal cord and in peripheral nociceptive neurons (Steenland et al., 2006; Kauer and Gibson, 2009) have been interpreted as showing involvement of TRPV1 in cognition, pain perception and in neuropsychiatric disorders (Di Marzo et al., 2008). Indeed, TRPV1 receptor in the central nervous system is a target for TRPV1-antagonist-mediated analgesia (Cui et al., 2006). In addition, TRPV1 knockout mice have reduced anxiety and conditioned fear responses (Marsch et al., 2007), reduced hippocampal long-term potentiation (LTP), and reduced long-term depression (LTD) (Gibson et al., 2008). Moreover, pharmacological inhibition of TRPV1 is known to increase anxiety-like behaviors in rodents (Micale et al., 2009; Aguiar et al., 2009). On the basis of the finding that neurogenesis is significantly reduced in TRPV1 and cannabinoid receptor 1 (CB1) double-knockout animals (*Cb1*$^{-/-}$, *Trpv1*$^{-/-}$), it has been postulated that TRPV1 is involved in neurogenesis (Jin et al., 2004).

Several studies have suggested that TRPV1 is involved in synaptic transmission, neurotransmitter release and plasticity (Kauer and Gibson, 2009; Maione et al., 2009; Li, H. B. et al., 2008; Marinelli et al., 2007; Starowicz et al., 2007b; Starowicz et al., 2008). Involvement of TRPV1 in glutamatergic synaptic transmission has been documented for rat sensory neurons and also for the input into dorsolateral periaqueductal gray neurons (Sikand and Premkumar, 2007; Medvedeva et al., 2008; Xing and Li, 2007). Similarly, activation of TRPV1 is necessary and sufficient to trigger LTD at glutamatergic synapses in the hippocampus and the developing superior colliculus (Gibson et al., 2008; Alter and Gereau, 2008; Maione et al., 2009). Capsaicin has been shown to alter synaptic transmission in the rat medial preoptic nucleus, a hypothalamic area that regulates body temperature (Kauer and Gibson, 2009; Karlsson et al., 2005). N-arachidonoyl-dopamine (NADA), an agonist for TRPV1, is known to modulate the presynaptic Ca^{2+} levels and transmitter release in the hippocampus (Huang et al., 2002; Starowicz et al., 2007b; Tóth et al., 2009; Köfalvi et al., 2007). Although all these reports support a function of TRPV1 at synapses, direct evidence for the presence of TRPV1 in synapses is lacking. It is also not clear whether TRPV1 is associated with presynaptic and/or postsynaptic structures. Moreover, the issues of TRPV1-mediated modulation of synaptic functions and transmission are poorly understood.

Previously, we reported that TRPV1 interacts with microtubules and regulates the function of growth cones by cytoskeletal reorganization (Goswami et al., 2004; Goswami et al., 2006; Goswami et al., 2007a; Goswami et al., 2007b). Expression of TRPV1 in DRG-derived F11 cells, a fusion cell line developed

from rat DRG neurons and mouse neuroblastoma cells, results in increased neuritogenesis and the formation of extensive filopodial structures (Goswami and Hucho, 2007). Surprisingly, most of these filopodia contain elevated levels of TRPV1 at their tips and morphologically resemble elongated club-shaped spines. In the present study we demonstrate that TRPV1 is present in pre- and postsynaptic structures, and that it is transported to synaptic sites by synaptic transport packets. We also provide evidence that TRPV1 regulates filopodial dynamics and vesicle recycling, processes that are important for synaptogenesis.

Results

TRPV1 localizes to the spines of primary cortical neurons and is present in synaptic protein preparations

On the basis of our previous work (Goswami and Hucho, 2007), we hypothesized the presence of TRPV1 in synapses. Primary cortical neurons were employed to test this hypothesis. Because the expression level of endogenous TRPV1 in these neurons was too low for immunocytochemical analysis, we expressed TRPV1 for 6 hours in cortical neurons and analyzed its localization. In spite of the short expression period, TRPV1 became enriched in distinct spots resembling synapses (Fig. 1A). To test whether these puncta represent dendritic spines carrying synapses, we co-stained TRPV1 with endogenous pre- and postsynaptic markers. TRPV1 colocalizes with endogenous pre- and postsynaptic marker proteins, including the active-zone protein Bassoon and postsynaptic elements such as GluR2-containing AMPA receptors, NMDA receptors and PSD95 (Fig. 1A,B). We also observed that TRPV1 colocalizes with ProSAP1 (also known as Shank2; a protein that is mainly present in the postsynaptic density) in distinct punctate spots (Fig. 1C). We also noted that TRPV1 localizes in both MAP2a/b-positive as well as MAP2a/b-negative neurites (Fig. 1D), indicating that TRPV1 is present in both the axon and dendritic structures. Altogether, these data indicate that TRPV1 colocalizes with both pre- and postsynaptic marker proteins in these structures, as visualized by confocal microscopy.

To verify that TRPV1 is associated with synaptic structures, we purified synaptic proteins from rat spinal cord, where expression of TRPV1 has been reported (Lewinter et al., 2004). We tested individual protein fractions for the presence of TRPV1 and by immunoblot analysis we detected TRPV1 in rat spinal-cord homogenate, the crude membrane fraction, synaptosomal fraction and also in the synaptic junctional protein fraction (Fig. 1E). TRPV1 immunoreactivity is enriched in the synaptic protein fractions and matched well with the molecular weight attributed to the monomeric TRPV1. Interestingly, we also observed immunoreactivities that matched with glycosylated (Fig. 1E, smeary appearance in lane 3) and dimeric TRPV1 in synaptosomes and in synaptic junctions, respectively (Fig. 1E). The purity of the fractions was further confirmed by probing the same fractions for PSD95 and synaptophysin (Fig. 1E).

Activation of TRPV1 alters spine morphology in cortical neurons

Previously, we reported that activation of TRPV1 elongated filopodial structures in F11 cells (Goswami and Hucho, 2007). Therefore, we tested whether brief activation of TRPV1 can also alter the spine morphology in cortical neurons. To achieve this objective, neurons were treated with NADA (0.2 μM, 3 minutes), an endogenous ligand of TRPV1 (Huang et al., 2002). We observed that a large number of spines developed from TRPV1-expressing neurons were elongated (Fig. 2A). Spines from neurons that did not express TRPV1 did not display morphological changes upon NADA application. To confirm that the NADA-induced spine elongation is indeed due to TRPV1 activation, we preincubated cortical neurons with the TRPV1-specific inhibitor 5′-iodoresiniferatoxin (5′I-RTX; 1 μM, 10 minutes) before applying NADA (0.2 μM, 3 minutes). Neither elongation nor morphological alteration of spines was observed in TRPV1-expressing neurons (Fig. 2B). We quantified and plotted the spine lengths in ascending order from neurons that express TRPV1 after the different drug treatments. A clear shift in the spine length after NADA treatment was observed when compared with the spines in control conditions or after NADA treatment in the presence of 5′I-RTX (Fig. 2C). The spines from NADA-treated neurons were longer (average length 3.37 μm, s.e.m. 0.16 μm) than those in non-stimulated control neurons (average length 1.84 μm, s.e.m. 0.1137 μm) (Fig. 2D). By contrast, spines from neurons that were pretreated with 5′I-RTX prior to NADA application were even shorter than the spines from non-stimulated control neurons (average length 1.28 μm, s.e.m. 0.626 μm). Interestingly, the significant (P~0.05) shortening of spines in this latter condition suggests that spontaneous tonic activation of TRPV1 might play a role in the regulation of spine length (discussed below). Our results suggest that activation of TRPV1 by NADA promotes spine elongation and that this can be blocked by 5′I-RTX.

TRPV1 and synaptic proteins are enriched at the tip of the elongated filopodial structures

Previously, we observed that the majority of the TRPV1-induced filopodial tips of F11 cells are club-shaped and therefore morphologically resemble the elongated dendritic spines developed from primary neurons (Goswami and Hucho, 2007). We therefore explored whether these club-shaped filopodial structures might indeed constitute synaptic sites. For further experiments, we used F11 cells as a test system (Platika et al., 1985). These cells reflect several properties of primary DRG neurons, but do not express TRPV1 endogenously. Thus, this cell line offers the possibility to study the effects of heterologously expressed TRPV1 on synaptogenesis.

As observed in our earlier experiments (Goswami and Hucho, 2007), expression of TRPV1-GFP induced massive filopodia development. In the current study, even when using low expression levels of TRPV1-GFP, we observed fluorescence along neurites and enrichment at the tip of filopodial structures within 6 hours. By contrast, when overexpressing soluble mCherry, we failed to observe such an enrichment of mCherry in filopodial structures (Fig. 3A; supplementary material Fig. S1), indicating the specificity of the TRPV1-GFP enrichment at the filopodial tips.

Furthermore, we tested whether TRPV1-positive filopodial tips contain synaptic proteins. To this end we expressed Bassoon-GFP (a presynaptic marker) or PSD-Zip45-GFP and GFP-PSD95 (markers for postsynaptic side) along with TRPV1. All three markers were highly enriched in TRPV1-induced filopodial tips (Fig. 3B), suggesting that TRPV1 accumulates in structures resembling both pre- and postsynapses. Previously, two presynaptic vesicular proteins, namely Snapin and synaptotagmin have been reported to interact with TRPV1 (Morenilla-Palao et al., 2004). Therefore, we assessed whether synaptic-vesicle markers also colocalize with TRPV1. Indeed, both Snapin-GFP and synaptophysin-GFP were found to colocalize with TRPV1 in

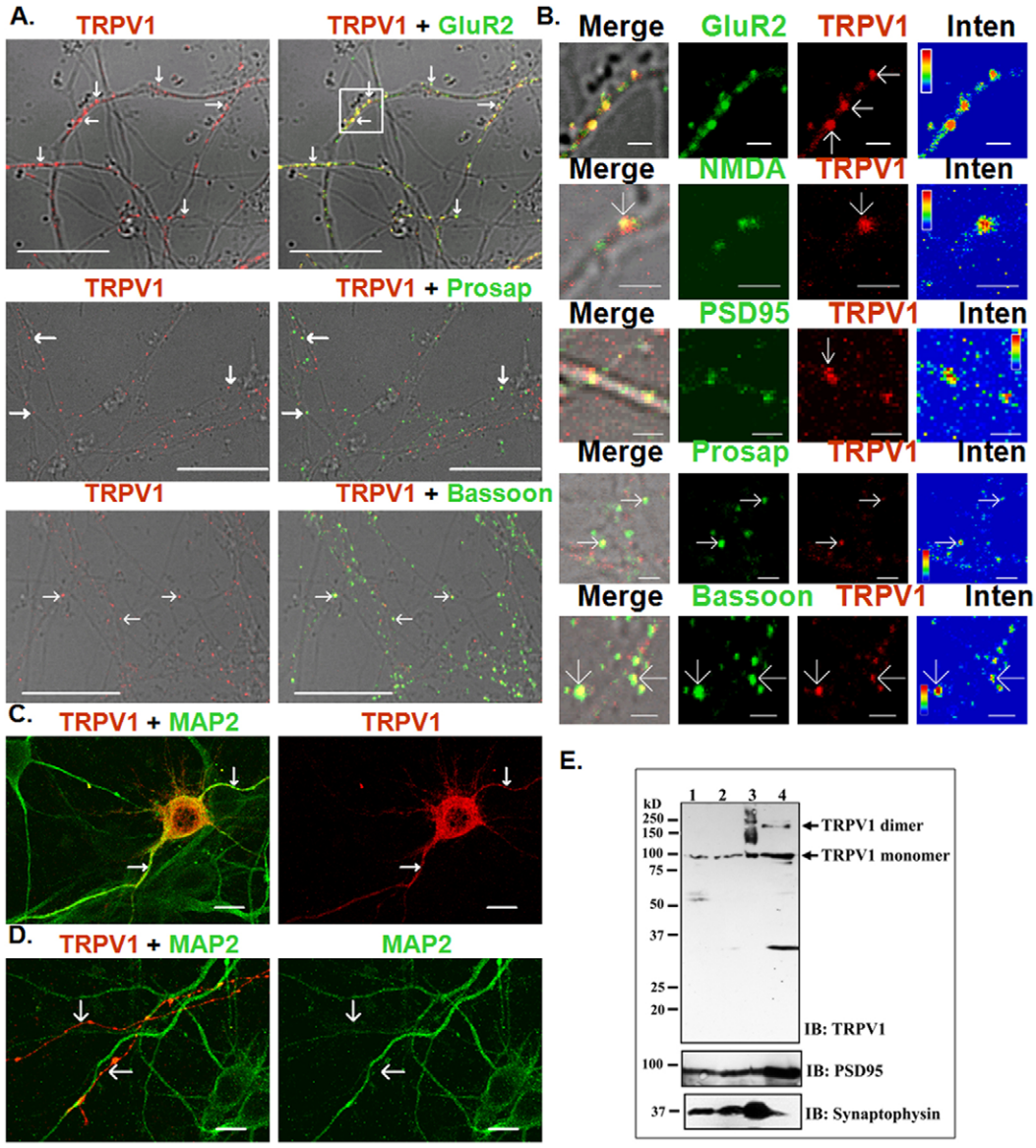

Fig. 1. TRPV1 is present at synaptic sites. (**A**) Images of cortical neurons transiently expressing TRPV1 at a low level. Neurons were immunostained for TRPV1 (red) and for GluR2 (green, top panel), ProSAP1 (Shank2; green, middle panel) or Bassoon (green, lower panel). The immunofluorescence images were superimposed to the phase-contrast images. TRPV1 localizes as distinct punctuate spots that colocalize with GluR2, ProSAP1 and Bassoon. Arrows indicate TRPV1-positive spots that colocalize with the other marker proteins. Scale bars: 10 µm. (**B**) TRPV1 colocalizes with both pre- and postsynaptic proteins. Enlarged areas of neurite mesh (as indicated by a white box in A) immunostained for TRPV1 (red) and different synaptic proteins (green) are shown. Merged images are superimposed to the phase-contrast images (left panel). Enrichment of TRPV1 in spines is shown in pseudocolor ('Inten'; right most panel). Arrows indicate the presence of TRPV1 in these spots. Scale bars: 2 µm. (**C**,**D**) TRPV1 localizes both in the axon and dendrites. Shown are the images of cortical neurons transiently expressing TRPV1. Neurons were immunostained for TRPV1 (red) and for MAP2 (green). Arrows indicate the TRPV1-positive neurites. Note that TRPV1 localizes both in MAP2-positive neurites (C) and TRPV1-negative neurites (D). Scale bars: 10 µm. (**E**) TRPV1 is present in synaptosomal fractions. Tissue homogenates from adult rat spinal cord (lane 1), membrane fraction (lane 2), synaptosomal fraction (lane 3) and synaptic junctional protein fraction (lane 4) were probed for TRPV1, PSD95 and synaptophysin. Arrows indicate monomeric and dimeric TRPV1. TRPV1 is enriched in synaptosomes and in synaptic junctions. Approximately 25-µg protein samples were loaded in each lane. The 37-kDa band at lane 4 is most probably a degradation product.

filopodial tips (Fig. 3B). The tips of spines as well as presynaptic terminals contain endocytic zones at which clathrin-mediated endocytosis takes place (Blanpied et al., 2002; Gundelfinger et al., 2003). Thus, we coexpressed TRPV1 and clathrin-GFP in F11 cells, which revealed that both recombinant proteins colocalize in filopodial tips (Fig. 3B). These results indicate that TRPV1-induced filopodial tips contain synaptic scaffold and vesicular proteins, suggesting that these tips can act as synaptic terminals.

To confirm that localization of TRPV1-GFP in filopodia is an active process, we performed fluorescence recovery after photobleaching (FRAP) experiments. We observed that TRPV1-GFP fluorescence recovers rapidly (within 3 minutes) in filopodia. Within individual filopodia, we noted both anterograde (Fig. 3C)

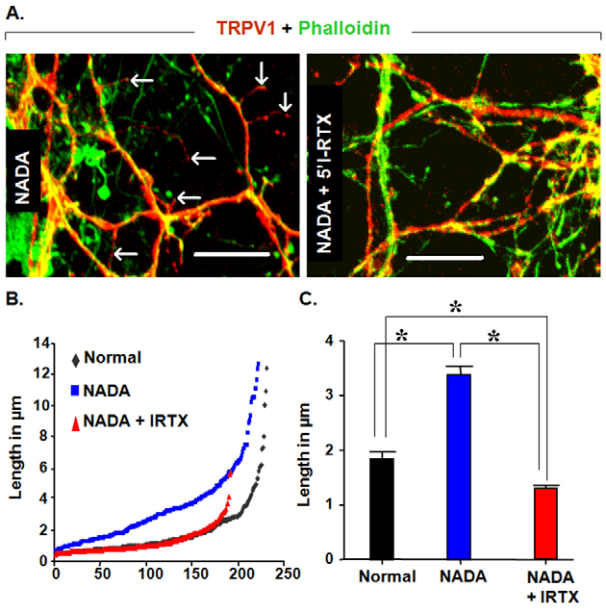

Fig. 2. TRPV1 affects spine length after activation. (**A**) Activation of TRPV1 alters the spine morphology of cortical neurons. Examples of cortical neurons expressing TRPV1 were stained for TRPV1 (red) and actin (green; stained with phalloidin). Neurons stimulated (3 minutes) by NADA (0.2 µM) or by NADA in the presence of the antagonist 5′I-RTX (1 µM) are shown. The arrows indicate elongated spines. Scale bars: 10 µm. (**B**) Spine lengths from cortical neurons expressing TRPV1 and treated with NADA (blue), NADA in the presence of 5′I-RTX (red) or unstimulated (black) were arranged in ascending order. Each spot indicate length of individual spines in *y*-axis. (**C**) The average length of spines from TRPV1-expressing neurons treated with NADA (blue; average 3.37 µm, s.e.m. 0.16 µm, *n*=223, five neurons), NADA in presence of 5′I-RTX (red; average 1.28 µm, s.e.m. 0.626 µm, *n*=193, seven neurons) or unstimulated (black; average 1.84 µm, s.e.m. 0.1137 µm, *n*=232, seven neurons) are shown ($P<0.0001$, unpaired one-tailed Student's *t*-test). Significant (*) differences are indicated.

and retrograde (not shown) movements of TRPV1-GFP in discrete packets after photobleaching, suggesting that TRPV1-GFP localization within filopodia is not due to passive diffusion within the membrane. Taken together, these results indicate that the enrichment of TRPV1 at the filopodial tips is specific and most probably is an active process.

TRPV1-enriched filopodial tips at sites of cell-cell contact contain synaptic proteins

Filopodia can establish cell-cell contacts that can either mature and become consolidated or can disappear again. Previously, we reported that TRPV1-enriched filopodial structures are found at established cell-cell contacts (Goswami and Hucho, 2007). To test whether these filopodia-based cell-cell contacts can contain synaptic marker proteins and TRPV1, we coexpressed TRPV1 with postsynaptic, presynaptic and synaptic vesicular proteins in F11 cells. Reconstructed three-dimensional (3D) images of these filopodia confirmed that cell-contact-forming filopodial tips contained TRPV1 as well as the postsynaptic proteins GFP-PSD95, PSD-Zip45-GFP or the presynaptic protein Bassoon-GFP (Fig. 4). Moreover, clathrin-GFP, Snapin-GFP, synaptophysin-GFP and synapsin-GFP were present at these contacts (Fig. 4), suggesting that filopodial tips can form consolidated synapse-like structures.

TRPV1 is transported to neurite endings and at filopodial bases by transport packets

If TRPV1 is a synaptic protein, then it will be transported within neurites by transport packets. We observed that, apart from some diffuse staining, TRPV1-GFP mainly appears as distinct puncta all along the neurites. These fluorescent structures containing TRPV1-GFP were variable in size and shape and were much larger than common transport vesicles. Therefore, we explored whether these structures represent the 'synaptic transport packets' (Ahmari et al., 2000), which are characterized by the presence of synaptic proteins as they transport synaptic components to their site of destination. To test this hypothesis, we expressed TRPV1 along with the synaptic-vesicle protein Snapin-GFP and performed immunostaining. We observed that TRPV1 and Snapin-GFP colocalize in punctate spots within long neurites (Fig. 5A). Similar co-distribution of postsynaptic scaffold proteins such as GFP-PSD95 or PSD-Zip45-GFP along with TRPV1 was also observed in such punctate spots (data not shown).

Because transport packets are mobile within neurites, we tested whether these TRPV1-GFP-containing spots are also mobile. To achieve these objectives, we coexpressed TRPV1-GFP and synaptophysin-mCherry in F11 cells and performed live-cell imaging (Fig. 5B). TRPV1-GFP colocalizes with synaptophysin-mCherry in neurites as distinct punctate spots. These spots also move fast and travel a long distance at a stretch. It was observed that these spots can move in both directions along neurites. The co-migration of TRPV1-GFP and synaptophysin-mCherry within the neurite corroborates the notion that these structures are indeed transport packets (Fig. 5B). Remarkably, these transport packets were frequently located at the base of short filopodia (Fig. 5C). There, they were observed to be stationary for several minutes to hours, especially the bigger units (~0.5 µm), which remained stable and static (either did not move at all or moved very little in both the directions). However, if moving and in close proximity to each other, then these bigger units often fused. For the movement of TRPV1-positive units, we determined a maximum velocity of 0.45 µm/second.

TRPV1-expressing cells reveal fast uptake of FM4-64 dye

Several reports suggest that agonists of TRPV1 stimulate neurotransmitter release (Li and Eisenach, 2001; Schmid et al., 1998; Xing and Li, 2007; Sikand and Premkumar, 2007; Medvedeva et al., 2008; Gibson et al., 2008; Alter and Gereau, 2008; Marinelli et al., 2007; Starowicz et al., 2007a). It is a well known fact that neurotransmitter release is associated with vesicle recycling. Therefore, we studied uptake of FM4-64 dye at TRPV1-positive sites.

We decided to test whether TRPV1-GFP-expressing F11 cells can incorporate the dye. Indeed, the uptake of FM4-64 dye was very fast. If used at the normally reported concentration of 0.1 µg/ml of final dye solution, the cells showed almost instant loading (often within 30 seconds). However, also after lowering the dye concentration to as low as 0.5 ng/ml, loading of FM4-64 in TRPV1-GFP-expressing populations was observed within a few (1-2) minutes (supplementary material Fig. S2A). At this concentration, mock-transfected control cells showed nearly no incorporation (supplementary material Fig. S2B).

FM4-64 is a lipophilic dye and the fast incorporation of this dye even in the absence of Ca^{2+} was quite unexpected. Therefore, we tested the specificity of the uptake. If the uptake is specific and actively driven it would have been possible to block this dye

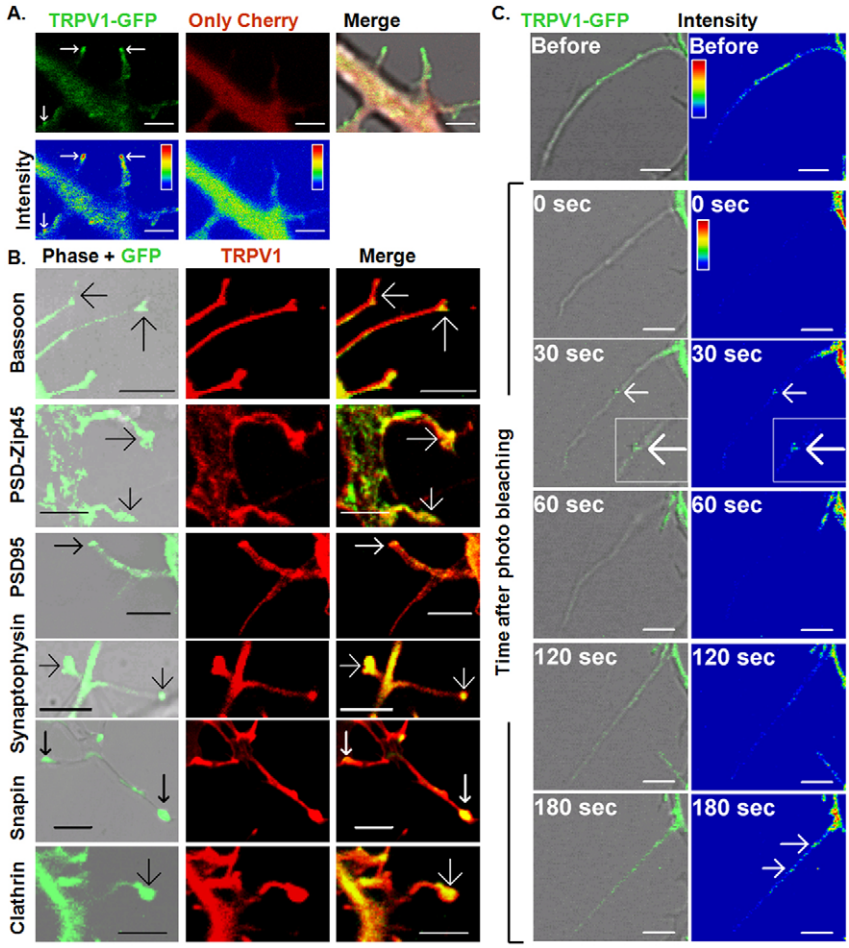

Fig. 3. TRPV1 localizes at filopodial tips. (**A**) Shown are the enlarged views of filopodia developed from a live F11 cell expressing TRPV1-GFP (green) or mCherry (red) at low levels. Specific enrichment of TRPV1-GFP (green) at filopodial tips (indicated by arrows) is observed, whereas mCherry is mainly restricted to the neurites. Merged fluorescence image superimposed with phase-contrast image is shown on the right side. The corresponding intensity profiles are provided in the lower part. Scale bars: 2 µm. (**B**) TRPV1 colocalizes with presynaptic, postsynaptic and synaptic vesicular proteins at filopodial tips. Images represent enlarged views of filopodial structures. TRPV1 (red) and different GFP-tagged synaptic markers (green) were expressed in F11 cells. In the left panel, fluorescence images are superimposed to the phase-contrast images. Arrows indicate the presence of synaptic-marker proteins at filopodial tips. Scale bars: 5 µm. (**C**) Fluorescence recovery after photobleaching (FRAP) of TRPV1-GFP within individual filopodia. In the left panel, fluorescence images are superimposed to the phase-contrast images. Corresponding intensities are provided in the right side. Arrows indicate the movement of discrete TRPV1-GFP particles within the filopodia (an enlarged view is provided in the 30-second inset). Scale bars: 2 µm.

uptake by pharmacological manipulation of the actin cytoskeleton, which plays an important role in membrane trafficking processes (Gundelfinger et al., 2003; Girao et al., 2008). Therefore, we explored whether disruption of the actin cytoskeleton can block uptake of the FM4-64 dye. Loading of FM4-64 was reduced upon pre-treatment of TRPV1-GFP-expressing F11 cells with cytochalasin D (supplementary material Fig. S3A), indicating that the uptake was indeed actin dependent. To further confirm the specificity, we monitored dye uptake at lower temperatures, which also blocks active endocytosis and therefore interferes with dye uptake. When added to TRPV1-GFP-expressing F11 cells at 4°C, the uptake of FM4-64 was almost undetectable (supplementary material Fig. S3B). Fluorescence-activated cell sorting (FACS) measurements were employed to quantify the effects. As shown in Fig. 6, a clear shift in FM4-64 uptake was observed in unstimulated TRPV1-GFP-expressing F11 cells when compared with the F11 cells that were either non-transfected or express GFP only. TRPV1-GFP-expressing cells incorporated 2.35-fold (P=0.0001) or 1.69-fold (P=0.00053) more FM4-64 as compared with F11 populations that were either non-transfected or expressed only GFP, respectively (Fig. 6B). Similarly, TRPV1-GFP-expressing cells showed a significant reduction (0.33-fold, P=0.0004) of dye uptake if these cells were treated with cytochalasin D. Cold treatment of TRPV1-GFP-expressing F11 cells also resulted in a 0.48-fold reduction (P=0.0014) in dye uptake as compared with unstimulated TRPV1-GFP cells. These cold-treated cells did not show a significant difference in comparison with the non-transfected cells (0.22-fold increase, P=0.2259). Uptake of FM4-64 dye varies in different other conditions also (supplementary material Fig. S4). From these results we conclude that the fast and differential uptake of FM4-64 dye in TRPV1-expressing cells reflects an active endocytotic process that is much enhanced by the presence of TRPV1.

TRPV1-transfected F11 cells take up FM4-64 at distinct sites enriched for TRPV1

In this study we also tried to identify the subcellular site of FM4-64 uptake in TRPV1-transfected F11 cells. Specific and rapid labeling (within 1-2 minutes) with FM4-64 was observed as distinct spots along neurites (Fig. 6C). Often these spots also contained TRPV1-GFP and appeared as donut-like structures resembling the topology of synaptic-vesicle clusters (see Discussion). These spots were mostly juxtaposed to the base of small filopodia and were clearly visible as distinct bright spots (Fig. 6C). In addition, FM4-64 loading was observed at elongated filopodia (Fig. 6D). We also explored whether the club-shaped filopodial tips can incorporate this dye. Indeed, a few (but not all) TRPV1-GFP-induced club-shaped filopodial tips contained FM4-64 (Fig. 6E; supplementary material Fig. S5A). Specific FM4-64 labeling was also observed at some areas of the cell body and growth cones (data not shown). The fast labeling of FM4-64 to limited cellular regions suggests that these specific structures harbor fast-recycling vesicles.

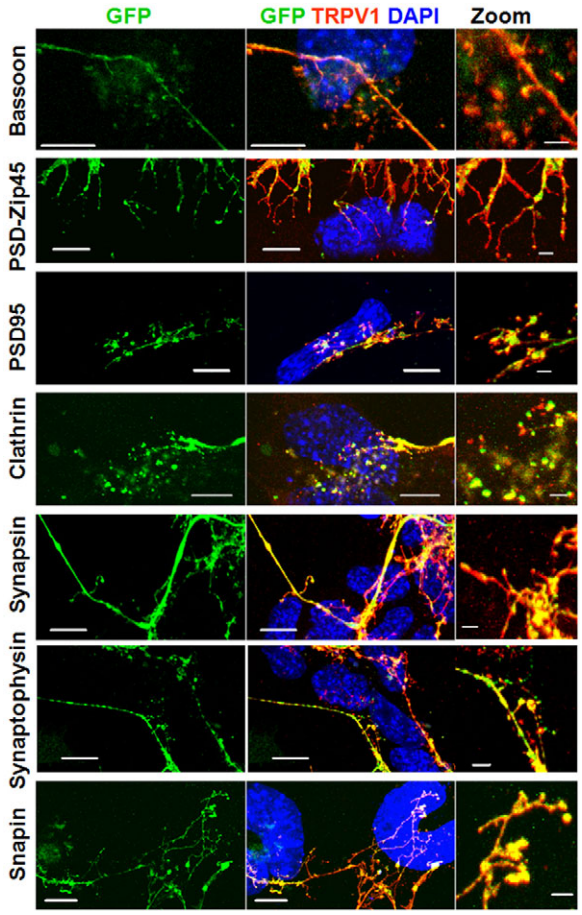

Fig. 4. TRPV1-enriched filopodial tips engaged in the formation of cell-cell contacts contain postsynaptic, presynaptic and synaptic vesicular proteins. TRPV1 (red) and different GFP-tagged synaptic marker proteins (green) were coexpressed in F11 cells and 3D-reconstructed images (from confocal *z*-sections, 0.5 µm) of neurites with filopodia engaged in cell-cell contact formation are shown. Scale bars: 5 µm. Enlarged view of the cell-cell-contact-forming filopodial structures are shown in right side. Scale bars: 2 µm.

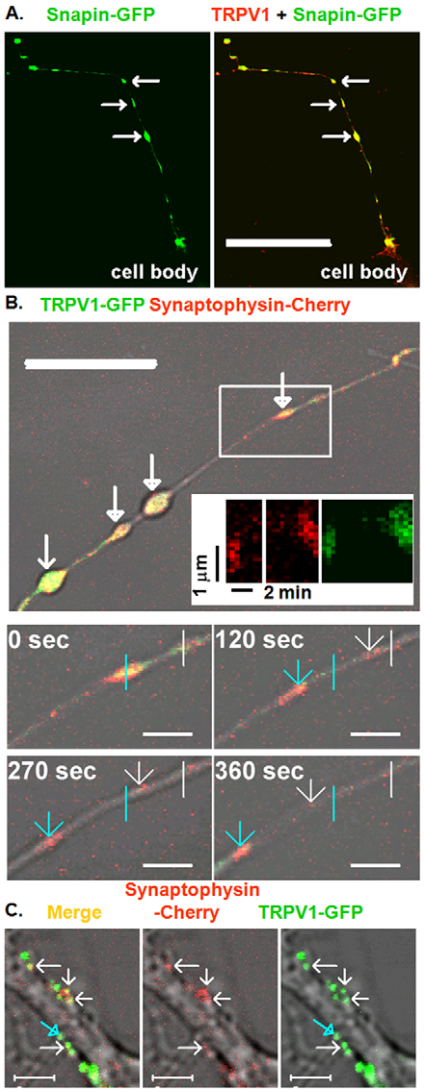

Fig. 5. TRPV1 is transported to the neuronal ends by transport packets. (**A**) Confocal images of a neurite demonstrating colocalization (indicated by arrows) of TRPV1 (red) with Snapin-GFP (green). Scale bar: 50 µm. (**B**) Live-cell confocal image depicting the colocalization of TRPV1-GFP (green) and synaptophysin-mCherry (red) within a neurite developed from an F11 cell. Scale bar: 10 µm. A kymograph analysis through a cross-section of this neurite is shown in the inset. Live time images of an enlarged area (indicated by a box) depicting the co-migration of TRPV1-GFP and synaptophysin-mCherry are shown below. Straight vertical lines (white and blue, respectively) indicate the initial positions of transport packets and arrows (white and blue, respectively) indicate the relative position of these packets at certain time-points. Scale bars: 2 µm. (**C**) Transport particles (indicated by white arrows) containing TRPV1-GFP (green) and synaptophysin-mCherry (red) paused at the inner surface of the neurites and often at the base of the filopodia (indicated by blue arrows). Fluorescence and phase-contrast images are superimposed. Scale bars: 5 µm.

TRPV1-activation-mediated filopodial elongation is due to rapid vesicle fusion

We demonstrated that NADA treatment resulted in a quick increase in spine length of cortical neurons (Fig. 2). Elongation of spines requires a rapid supply of lipid membranes. Therefore, we hypothesized that filopodial elongation by TRPV1 activation should be accompanied by rapid vesicle fusion delivering membrane components. To test this hypothesis we applied NADA to TRPV1-GFP-expressing F11 cells. This treatment caused an initial reduction in FM4-64 intensity and resulted in the formation and/or elongation of filopodia soon after (Fig. 7A). We also observed that the membrane area at the filopodial bases increased over time after TRPV1 activation, especially during the filopodia-elongation phase (Fig. 7B, upper images). This increased membranous region contained TRPV1-GFP and was labeled with FM4-64 dye during and after the filopodia-elongation phase (Fig. 7B, lower images). Taken together, these results suggest that TRPV1 activation induces rapid vesicle fusion at the filopodial base and results in the elongation of filopodia.

TRPV1 activation results in exocytosis

During this study we often observed that addition of Ca^{2+} (1 mM) to the Hanks' balanced salt solution (HBSS) buffer resulted in rapid loss of FM4-64 staining (supplementary material Fig. S4A). Thus, we hypothesized that Ca^{2+} influx through TRPV1 (e.g. activation of TRPV1) might result in exocytosis, i.e. unloading of

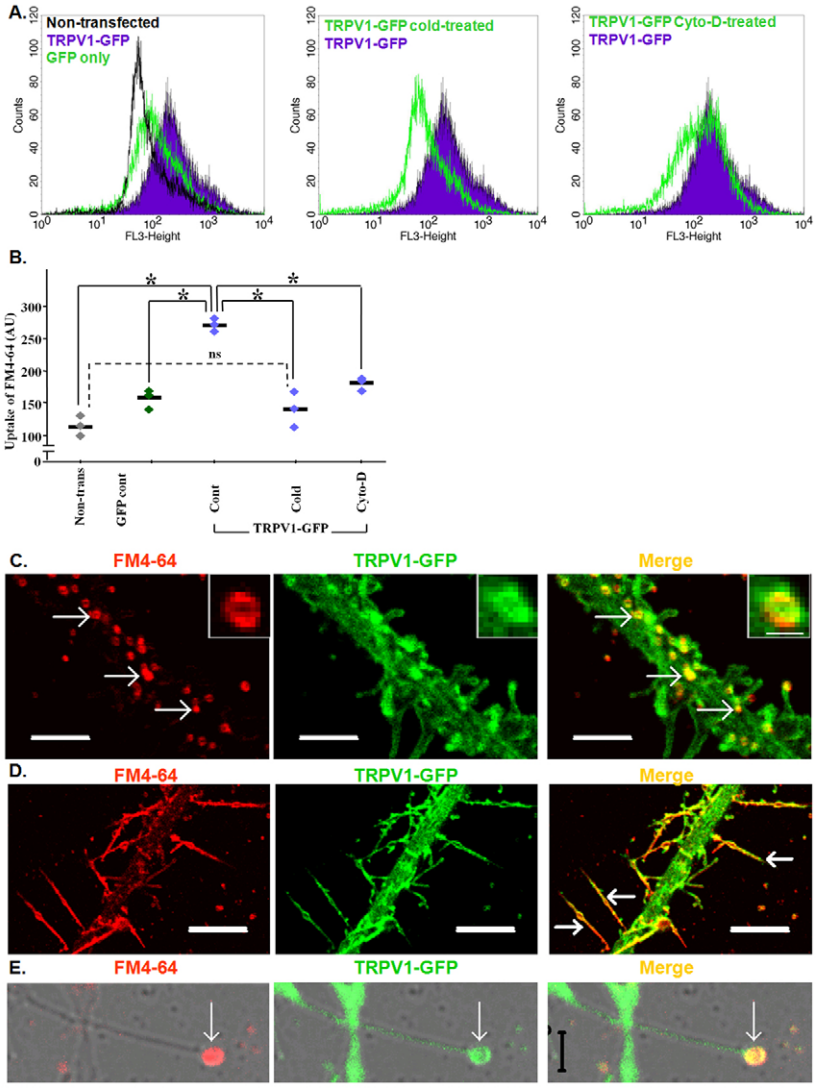

Fig. 6. TRPV1 modulates cellular uptake. (**A**, left panel) Comparative FACS profiles showing uptake of FM4-64 by TRPV1-GFP (violet), GFP only (green) or non-transfected (black) F11 populations in untreated conditions. (Middle panel) A similar comparison between untreated (violet) and cold-treated (green) F11 population expressing TRPV1-GFP is shown. (Right panel) A Cyto-D-treated TRPV1-GFP population (green) takes less dye when compared with the untreated TRPV1-GFP population (violet). (**B**) Quantification of the FM4-64 uptake (arbitrary units) in different conditions. Significant (*) or non-significant (ns) differences are indicated (0.05 significance level, Student's *t*-test, two populations). (**C-E**) Shown are the confocal images demonstrating TRPV1-GFP (green) colocalization with FM4-64 (red) in specific subcellular regions. (C) Presence of active zones (indicated by arrows) as distinct spots within the neurite is shown. An example of a donut-like spot is shown in the enlarged image in the corner. Scale bars: 5 µm. (D) Uptake of FM4-64 at the filopodial stalks is indicated by arrows. Scale bars: 10 µm. (E) Example of a club-shaped filopodial structure labeled with FM4-64 at the tip (arrows). Fluorescence and phase-contrast images are superimposed. Scale bar: 2 µm.

FM4-64. To test this hypothesis, we first added NADA for 4 minutes to TRPV1-GFP-expressing F11 cells in the presence of Ca^{2+} and then added FM4-64 dye. Just after addition of the dye, cells expressing TRPV1-GFP incorporated FM4-64 dye to a much lower extent than nearby cells that were either not transfected or contained trace amounts of TRPV1-GFP (supplementary material Fig. S4B). Moreover, TRPV1-GFP-positive cells showed a rapid loss of FM4-64, even in continuous presence of FM4-64 in the bath solution; after a few minutes virtually no staining remained in these TRPV1-GFP-positive cells. By contrast, TRPV1-GFP-negative cells remained strongly stained. Because, in the absence of agonists, TRPV1-transfected cells displayed enhanced endocytotic activity, we therefore conclude from these data that TRPV1 activation shifts membrane cycling towards exocytosis.

PKC-dependent exocytosis was described as a mode of potentiation of TRPV1 (Morenilla-Palao et al., 2004; Mandadi et al., 2006). Therefore, we speculated that PKC activation should induce unloading of FM4-64 dye in TRPV1-GFP-expressing F11 cells. Indeed, upon addition of phorbol 12-myristate 13-acetate (PMA; activator of PKCs), we observed fast FM4-64 loading in TRPV1-GFP-enriched neurites, but the intensity of FM4-64 signal at these structures decayed quickly (within 1-2 minutes) even in the continuous presence of dye in the bath (supplementary material Fig. S4B). This suggested a rapid exocytosis in response to PMA treatment either by PKC activation or by activating other phorbol-ester-sensitive processes, e.g. the activation of the priming factor Munc13 (Rhee et al., 2002).

To confirm these observations quantitatively, we compared FM4-64 uptake in unstimulated and stimulated TRPV1-GFP-expressing F11 populations by FACS measurements. We observed a clear reduction of FM4-64 quantity when TRPV1-GFP-expressing cells were stimulated with NADA or PMA (Fig. 7C); both NADA and PMA treatment resulted in significant reduction (0.46-fold, P=0.00015 and 0.44-fold, P=0.00014, respectively) as compared with the unstimulated TRPV1-GFP populations (Fig. 7D). These results indicate that TRPV1 activation indeed induces exocytosis.

Discussion

In this study we demonstrate the physical presence of TRPV1 in synaptic structures, such as in the spines of primary neurons and in biochemically prepared synaptosomes. Similarly, in DRG-neuron-derived F11 cells, TRPV1 physically colocalized with synaptic markers at filopodial tips. On the basis of structure,

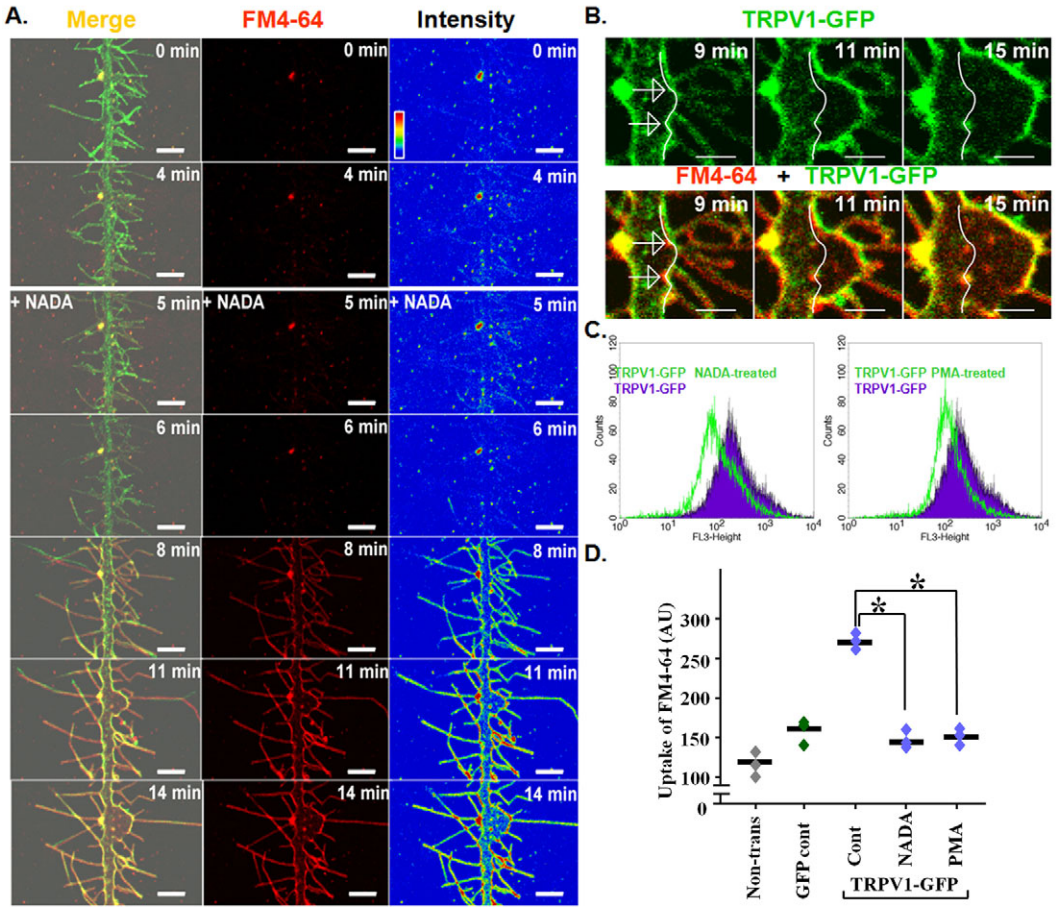

Fig. 7. Activation of TRPV1 results in rapid vesicle fusion resulting in elongation of filopodia and exocytosis. (**A**) Time-series images of a neurite developed from an F11 cell expressing TRPV1-GFP (green). FM4-64 (red) was added at *t*=0 minutes. Several filopodia emerge and elongate upon addition of NADA (0.2 µM). The corresponding FM4-64 signal and the intensity are provided in the middle and right panels, respectively. Scale bars: 5 µm. (**B**) An enlarged area of the filopodial bases depicting details of TRPV1-GFP and FM4-64 fluorescence in different time frames. Arrows indicate the FM4-64-labelled spots at the submembranous regions. With time the membranous border at the filopodial bases increases, indicating rapid fusion of vesicles (white line indicates the original position of the membranous border). Scale bars: 2 µm. (**C**) FACS profiles demonstrating the comparative uptake of FM4-64 in a TRPV1-GFP-expressing F11 population in unstimulated condition (violet) and after stimulation (green). The TRPV1-GFP-expressing population looses FM4-64 dye when treated with NADA (left side) or PMA (right side). (**D**) Quantification of FM4-64 uptake (arbitrary units) in different conditions. Significant (*) differences are indicated (0.05 significance level, Student's *t*-test, two populations).

molecular composition and function, our work indicate that these filopodial structures resemble 'synapses' or 'hemisynapses' because they contain clusters of receptors associated with signaling and scaffolding molecules as well as with release-competent synaptic vesicles (Craig et al., 2006). These structures contain postsynaptic as well as presynaptic markers. Finally, we showed that TRPV1 is involved in the regulation of membrane-recycling events such as endocytosis and exocytosis.

It has been shown previously that members of the TRPC family interact with synaptic proteins, are present in synaptic structures and are involved in neuronal network formation (Goel et al., 2002; Singh et al., 2004; Gomez, 2005; Li et al., 2005; Montell, 2004; Shim et al., 2005; Wang and Poo, 2005). Also, TRPM7 and TRPV4 have been detected in small synaptic-like vesicles and in spines (Brauchi et al., 2008; Shibasaki et al., 2007). Our data, together with accumulating reports of TRPV5, indicate a more general role for TRPV channels in vesicle fusion (Lambers et al., 2007).

But is TRPV1 also involved in the process of neuronal network formation? Our data and other reports suggest several cases where TRPV1 can be involved in network formation. TRPV1 is expressed throughout the period of establishment and fine-tuning of neuronal connections, even at early embryonic stages when there is no synaptogenesis (Hjerling-Leffler et al., 2007; Funakoshi et al., 2006; Goswami et al., 2007b). Ectopic expression of TRPV1 results in increased neuritogenesis and a large extent of filopodia production (Goswami and Hucho, 2007). Furthermore, TRPV1 regulates the morphology and motility of neuronal growth cones (Goswami et al., 2007b; Goswami and Hucho, 2008). Activation of TRPV1 results in the retraction of growth cones and formation of varicosities (Goswami et al., 2007b), bulge-like structures along neuronal axons where synaptic vesicles, mitochondria and ER accumulate (Pannese, 1994). These varicosities are able to form synaptic contacts when touching other cells or neurites (Pannese, 1994). They can also play a role in non-synaptic communication by releasing neurotransmitters directly (Zhu et al., 1986; Vizi et al., 2004). In addition, several endogenous substances, such as endocanabinoids, anandamide and other lipid derivatives, act on TRPV1 and have well-established roles in modulation of neuronal

hardwiring and synaptic functions (Berghuis et al., 2007; Di Marzo, 2008).

If TRPV channels are involved in the processes of neuronal wiring and communication, disruption of a TRPV gene should results in distinct neurological phenotypes. Indeed, there are several indications for this. TRPV1 knockout mice reveal changes in behavior and LTD (Marsch et al., 2007; Gibson et al., 2008; Kauer and Gibson, 2009). In humans, a mutation has been described potentially affecting TRPV1 and/or TRPV3 through a de novo balanced chromosomal translocation (Walter et al., 2004). Clinical features of this mutation include an increased head size, severe speech and vision defects, and mental retardation (MR), a phenotype potentially caused by deficits in neuronal development. One recurrent theme in MR includes problems of neuronal connectivity, in particular a reduction in the number of and increased length of dendritic spines (Newey et al., 2005). Our data suggesting that TRPV1 plays a role in the development of neuritic protrusions such as spines and varicosities would be consistent with such a morphological phenotype.

Despite accumulating evidence for a role of TRPV1 in synaptic function, its presence in synaptic structures has not been shown so far. Beyond its mere presence we now demonstrate that TRPV1 shares remarkable features with proteins that are involved in synaptic processes, both in terms of distribution as well as dynamic behavior. Within neurites, TRPV1 is present in large accumulations, which are mostly immobile but move at times. These properties fit well to the mode of transport of synaptic proteins by 'transport packets' (Sabo et al., 2006). Recently it has been demonstrated that the pause sites of these transport packets are predefined, mostly at the sites of the potential synapse formation (Sabo et al., 2006). These transport packets are present in filopodia and in areas that are involved in spine formation (Ahmari et al., 2000; Nakata et al., 1998; Marrs et al., 2001; Matus, 2001; Sabo and McAllister, 2003; Okabe et al., 1999; Roos and Kelly, 2000). These units are defined by the presence of synaptic marker proteins (Greka et al., 2003; Morenilla-Palao et al., 2004; Singh et al., 2004). In agreement with the above observation, we now provide evidence that, within the neurites and filopodia, TRPV1 colocalizes with several synaptic proteins. It also co-migrates with synaptophysin. Immobile transport packets containing TRPV1-GFP and synaptophysin are mostly present at the inner surface of the neurites and also at filopodial bases. Another important property of transport packets is the presence of both endocytotic and exocytotic markers (Sabo et al., 2006). Indeed, we also provide evidence that extensive membrane recycling occurs at TRPV1-containing structures, as indicated by fast FM4-64 loading and unloading; this finding is supported by the recently reported interaction with synaptic vesicular proteins, namely with synaptotagmin IX and Snapin (Morenilla-Palao et al., 2004).

On the basis of the FM4-64 labeling in living cells, we showed that the filopodia of TRPV1-expressing cells can behave similar to active zones. Presence of FM4-64 was visible at the base and all along the stalk of the filopodia, indicating the presence of fast recycling vesicles there. In some cases we even detected multiple transport packets loaded with FM4-64 within the TRPV1-positive filopodial shaft (supplementary material Fig. S5A). This observation is in accordance with the organization of the endocytotic machinery lateral to the actual synapse in dendritic spines as reported earlier (Racz et al., 2004). At the filopodial bases, the FM4-64-labelled TRPV1-GFP-containing structures mostly appeared as donut-like units. The shape, size (around 1 μm in diameter) and properties of these units resemble clusters of synaptic vesicles in other systems (Wimmer et al, 2006; Kittel et al., 2006). For example, labeling of FM1-43 dye in these structures is similar to that in the donut-like units at the *Drosophila* neuromuscular junction (Verstreken et al., 2008), which contain fast-recycling vesicles (Kittel et al., 2006; Atwood, 2006; Banting et al., 1998; Wimmer et al. 2006). However, unlike these donut-like units or elongating filopodial shaft, many of the club-shaped filopodial structures generally showed no labeling at the resting stage, and presence of FM4-64 at the tip was rare. The reason for this is not clear. It might be due to the lack of considerable amount of polymerized actin there (Goswami and Hucho, 2007), which is essential for vesicle recycling (Girao et al., 2008).

From our study it is not clear whether a direct correlation exists between the levels of FM4-64 uptake and TRPV1-GFP expression. Our FACS analysis indicates that individual cells belonging to the TRPV1-GFP-expressing population showed a mixed phenotype, i.e. very high to very low level of FM4-64 uptake. Generally, cells expressing a higher level of TRPV1-GFP took up less FM4-64 (supplementary material Fig. S6). Our microscopic studies also revealed that cells that were either non-transfected or expressed low amounts of TRPV1-GFP took up more FM4-64 than nearby cells that expressed high levels of TRPV1-GFP. It is not clear how TRPV1-GFP actually controls cellular uptake and release of FM4-64 in a cell population. It is possible that TRPV1 influences trafficking of exo- and endocytic vesicles, which might regulate the release of neuro-active substances. Such released substances might induce paracrine signaling to non-transfected cells present in the same population and thus might influence their FM4-64 uptake. Another possibility is that the presence of TRPV1 at low levels accompanied by 'spontaneous tonic activation' increases the basal Ca^{2+} levels. This 'spontaneous tonic activation' might stimulate the bulk endocytosis, a process that also involved in maintaining the filopodial length and spine morphology. In this regard, recent reports that demonstrate that antagonists of TRPV1, such as 5′I-RTX, produce opposite effects, indicating that tonic activation of TRPV1 in central neurons is functionally important, are of interest (Marinelli et al., 2008; Starowicz et al., 2007a; Maione et al., 2009).

Whereas neuronal loading of FM4-64 by classical methods is slow and needs stimulation, the uptake of FM4-64 in TRPV1-GFP-expressing F11 cells is very fast and is activity independent. However, the uptake is sensitive to disruption of the actin cytoskeleton or blockade of membrane cycling by exposure to low temperature. These results are in concordance with a recent report demonstrating that neuronal growth cones incorporate FM4-64 within 1 minute and this uptake is sensitive to disruption of the actin cytoskeleton and low temperature (Bonanomi et al., 2008). Similarly, fast and activity-independent uptake of FM4-64 has been reported for cortical astrocytes (Li, D. et al., 2008). We also show that activation of phorbol-ester targets such as PKCs and/or Munc13 result in fast decay of the FM4-64 signal, even in presence of dye in the bath solution. It indicates that activation by PMA induces rapid exocytosis. This observation agrees with the fact that PKCs activate and/or re-sensitize TRPV1 by recruiting more functional TRPV1 into the membrane (Mandadi et al., 2006; Morenilla-Palao et al., 2004). Moreover, it also agrees with the previous observations that TRPV1 activation leads to the release of different neurotransmitters, often in a PKC-dependent manner (Li and Eisenach, 2001; Schmid et al., 1998; Schicho et al., 2005; Bernardini et al., 2004; Morenilla-Palao et al., 2004; Marinelli et

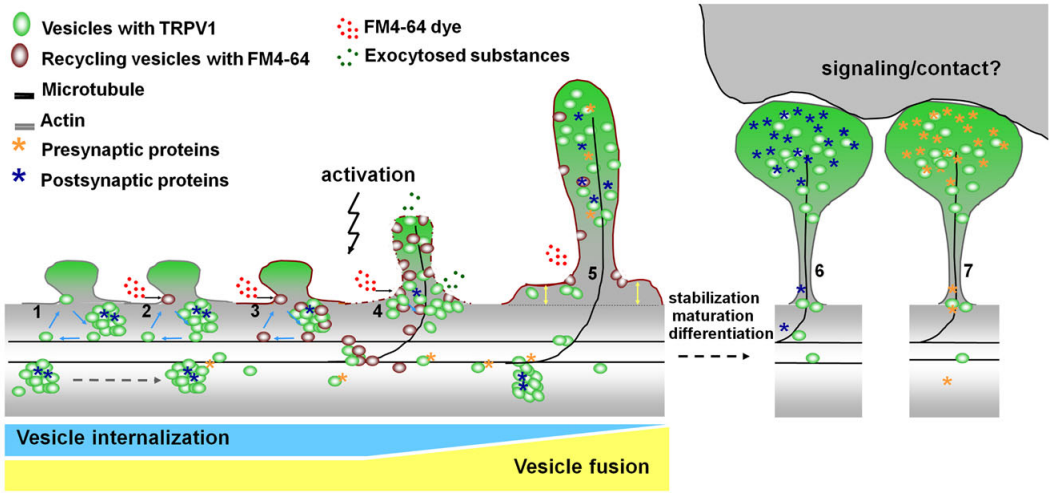

Fig. 8. Model for the involvement of TRPV1 in synaptogenesis. Mobile (indicated by a dashed arrow) transport packets containing TRPV1 pause at the inner surface of neurites (stage 1) and these packets have recycling vesicles (indicated by blue arrows). Addition of FM4-64 thus quickly labels these donut-like fast-recycling vesicles (stages 2 and 3). The vesicles fuse at the base of the filopodial structure and all along the filopodial stalk upon activation of TRPV1 (stage 4). Rapid vesicle fusion leads to the elongation of filopodial structures and often ballooning (indicated by bi-directional yellow arrows) of the filopodial base (stage 5). Chemical signaling and/or contacts might stabilize some of these filopodia, resulting in maturation of these structures that allows them to either differentiate as postsynaptic (stage 6) or presynaptic entities (stage 7).

al., 2007; Starowicz et al., 2007a). In this regard, TRPV1 activation might promote vesicle fusion by inducing direct Ca^{2+} influx. Alternatively, TRPV1 might act directly on the priming apparatus for synaptic-vesicle fusion, which is also a phorbol-ester-dependent event (Rhee et al., 2002).

Vesicular release and re-uptake are important features of functional synapses. Recent data suggested that TRP channels are involved in vesicle recycling. In PC12 cells, fusion of small synaptic-like vesicles is regulated by TRPM7 (Brauchi et al., 2008). Similarly, TRPV1-expressing F11 cells can rapidly incorporate FM4-64 at most of their filopodial structures, suggesting the presence of recyclable vesicles. Moreover, fast elongation of filopodial structures indicates intra-filopodial vesicle transport and fusion to supply lipids for the enlarging plasma membrane. On the basis of colocalization with synaptic and vesicular proteins, live-cell imaging of TRPV1-GFP with synaptophysin-mCherry, and loading-unloading experiments with FM4-64 dye, we propose that TRPV1 modulates synaptogenesis (Fig. 8) and/or synaptic maturation. TRPV1 colocalizes with immobile synaptic and recycling vesicles within neurites, which mostly act as putative synaptic sites. We propose that, owing to TRPV1 activation, more of these recyclable vesicles traffic into the filopodial shaft from the filopodial bases and some of them fuse with the filopodial membrane. In agreement with this hypothesis, we observed co-migration of TRPV1-GFP with synaptophysin-mCherry within the filopodia, especially during the elongation phase after NADA treatment (supplementary material Fig. S5B). These results are in agreement with the fact that filopodia are preferentially extended from synapses containing clusters of synaptic proteins (Panzer et al., 2006) and also with a report that NADA induces transmitter release (Marinelli et al., 2007).

It is intriguing to know why an FM4-64 signal all along the filopodial length is maintained long after NADA treatment. It is possible that some FM4-64 dye becomes trapped non-specifically within the filopodial membrane to sustain the signal. Involvement of enzymes regulating endovanilloid metabolism, secondary metabolites of NADA and other receptors might also contribute to the FM4-64 uptake in these structures in a more complex manner. For example, the presence of enzymes controlling endovanilloid biosynthesis and/or degradation is known to vary in different parts of the brain and subtype of the neurons, as well as in different compartments of neurons (Cristino et al., 2008). Moreover, secondary metabolites of NADA are known to affect TRPV1 (Rimmerman et al., 2009). Because NADA is known to activate also the CB1 receptor (although at much higher concentrations) (Sagar et al., 2004; Bisogno et al., 2000), involvement of CB1 in some of these NADA-mediated effects cannot be ruled out completely.

Several electrophysiological studies have demonstrated an effect of TRPV1 in synaptic transmission. Nevertheless, from these studies it is still not clear whether TRPV1 is present in pre- or postsynaptic areas. Presence of TRPV1-like immunoreactivity has been detected at the photoreceptor synaptic ribbons of goldfish and zebrafish retinas, suggesting a presynaptic localization of TRPV1 (Zimov and Yazulla. 2004). In this study we demonstrated that TRPV1-positive filopodia were present at sites of cell-cell contact as visualized by confocal microscopic images. Although we have not studied these contact sites at the ultrastructural level, we show that the filopodial tips at the contact sites contain presynaptic, as well as postsynaptic and synaptic vesicular proteins, indicating that such structures can potentially develop into either pre- or postsynaptic units. We observed that, in cortical neurons, TRPV1 is present in both MAP2- and Tau-positive neurites (data not shown). These observations are in high accord with previous reports indicating that functional TRPV1 is present in both pre- and postsynaptic regions (Valtschanoff et al., 2001; Doyle et al., 2002; Cristino et al., 2006). Our results also fit with a previous report that TRPV1 colocalizes with endovanilloid regulatory enzymes at pre- and post-synaptic regions, especially in the hippocampus and the cerebellum (Cristino et al., 2008). What determines the differentiation of TRPV1-containing filopodia to be pre- or postsynaptic identities remains as an intriguing question.

Materials and Methods

Reagents and antibodies

Affinity-purified rabbit polyclonal antibodies against TRPV1 were purchased from Alomone (Jerusalem, Israel) and Affinity BioReagents (Golden, CO). Mouse monoclonal anti-PSD95 (Stressgen), anti-GluR2 (Chemicon), anti-NMDA-receptor-2B (Affinity BioReagents, Clone NR2B), anti-synaptophysin (Stressgen), anti-MAP2 (Sigma-Aldrich) and anti-Bassoon (Synaptic System) antibodies were purchased from the above-mentioned sources, respectively. Alexa-Fluor-594-labelled anti-rabbit secondary IgG, Alexa-Fluor-488-labelled anti-rabbit secondary IgG, Alexa-Fluor-488-labelled anti-mouse secondary IgG, Alexa-Fluor-488-labelled phalloidin and the FM4-64 dye were purchased from Molecular Probes (Invitrogen, Karlsruhe, Germany). The antiserum against ProSAP1 was described before (Boeckers et al., 1999). HBSS buffer without Mg^{2+} and Ca^{2+} was purchased from GIBCO. NADA, 5′ I-RTX and PMA were purchased from Sigma Aldrich (Deisenhofen, Germany).

Constructs

Expression of TRPV1 and TRPV1-GFP constructs were conducted as described previously (Goswami et al., 2004; Goswami et al., 2007b). For expression of clathrin light chain (NM_001080385) tagged with GFP, the coding region was amplified by PCR (FP 5′-ATAGATCTATGGCCGAGTTGGATCC-3′, RP 5′-TAGTCGA-CTCAGTGCACCAGGGG-3′) from the mouse brain cDNA library (Invitrogen, Karlsruhe, Germany). The amplified cDNA fragment was inserted into the *Bgl*II and *Sal*I restriction sites of pEGFP-C1 vector (Clontech). GFP-PSD95 construct (prepared at David Bredt's laboratory, UCSF, CA) (Qin et al., 2001), PSD-Zip45-GFP (Okabe et al., 2001) and Snapin-GFP (Chen et al., 2005) constructs were kind gifts from M. E. Dailey (Department of Biological Sciences, University of Iowa, IA), Shigeo Okabe (School of Medicine, Tokyo, Japan) and B. L. Firestein (Rutgers University, New Brunswick, NJ), respectively. EGFP–Bassoon(96-3938) construct was described earlier (Dresbach et al., 2006). The synaptophysin-mCherry construct and synapsin-I–EGFP construct were kind gifts from Anna Fejtova with permission from Thomas Dresbach (University of Heidelberg, Heidelberg, Germany) and T. A. Ryan. (Department of Biochemistry, The Weill Medical College of Cornell University, NY), respectively. For expression of soluble mCherry, pmCherry-C1 vector (Clontech) was used.

Cell culture and transfection

F11 cells were cultured in Ham's F12 medium (Invitrogen, Karlsruhe, Germany) supplemented with 20% fetal calf serum (FCS; Invitrogen, Karlsruhe, Germany) and glutamate. Cells were maintained in a humidified atmosphere at 5% CO_2 and 37°C. For transient transfection, Lipofectamine with PLUS Reagent (Invitrogen, Karlsruhe, Germany) was used according to the manufacturer's instructions. Serum-free Opti-MEM media (Invitrogen) were used for transfection.

Primary neuronal culture

Primary cortical neurons were isolated as described previously (Brewer et al., 1993). Briefly, cortices were isolated from mouse brains (NMRI strain) on embryonic day 14 (E14), pooled and mechanically dissociated into a single-cell suspension in Neurobasal media (Invitrogen) supplemented with B27 (2%; Invitrogen) and 500 µM glutamine (Lonza). Subsequently, the cells were plated on poly-D-lysine- (Sigma) and laminin (Invitrogen)-coated glass coverslips in 12-well plates at a density of approximately 1×10^5 cells per well. For transient expression, primary cortical neurons were transfected at day 7 after plating in vitro with 1 µg DNA and 2 µl Lipofectamine 2000 (Invitrogen) per well (of 12-well plate) and subsequently fixed with 2% PFA.

Subcellular fractionation

Subcellular fractions (from six adult rat spinal cords) were prepared as described before for rat brain tissue (Wyneken et al., 2001). In brief, spinal-cord tissue was homogenized in buffer containing 5 mM HEPES, 320 mM sucrose and pH 7.4, with a Potter S (B. Braun, Melsungen, Germany) by 12 strokes at 1000 ***g***. Nuclei and cell debris were spun down at 1000 ***g*** for 10 minutes. The postnuclear supernatant was then centrifuged at 12,000 ***g*** resulting in a crude membrane fraction in the pellet. This pellet was resuspended and loaded on a sucrose density gradient with the following steps: 0.85 M, 1.0 M, 1.2 M. After centrifugation for 2 hours at 75,000 ***g***, synaptosomes were harvested at the 1.0/1.2 M interface. Synaptosomes were exposed to hypo-osmotic shock and the resulting membranes were spun down at 32,000 ***g***, resuspended and separated using another sucrose-gradient centrifugation under the same conditions as above. Synaptic junctions were harvested at the 1.0 M/1.2 M interface. Protein content was determined using a BCA assay (Pierce/Thermo).

Immunoblot

To perform immunoblot analysis, approximately 25 µg protein were loaded in each lane and further separated by SDS-PAGE (10%), then transferred to a PVDF membrane (Millipore) by semidry electroblotting. The membranes were blocked with 5% non-fat milk in TBS-T (20 mM Tris, 150 mM NaCl, 0.1% Tween-20) buffer followed by incubation with the primary antibodies overnight at 4°C. Horseradish-peroxidase-conjugated secondary antibodies (GE Healthcare/Amersham Biosciences, Freiburg, Germany) and the ECL detection system (Pierce and GE Healthcare/Amersham Biosciences, Freiburg, Germany) were used for the visualization of the immunoreactivity.

Immunocytochemistry and live-cell imaging

For immunocytochemical analysis, cells were fixed with 2% PFA for 5 minutes if not mentioned otherwise. To avoid morphological changes due to PBS wash, in some experiments an equal volume of 4% PFA was carefully added to the medium without disturbing the cell culture. Fixed cells were permeabilized with 0.1% Triton X-100 in PBS for 5 minutes, quenched with 2% glycine in PBS and blocked with 5% normal goat serum. All primary antibodies were used at 1:1000 dilution and were incubated for 1 hour at room temperature in PBST buffer (PBS with 0.1% Tween 20). All images were taken on a confocal laser-scanning microscope (Zeiss LSM Meta 100 M) with a 63× objective and analyzed with the Zeiss LSM image-examiner software. For live-cell imaging, cells grown on a glass coverslip were taken in the live-cell chamber and imaged at room temperature (25°C).

Labeling of FM4-64

FM4-64 dye was used to label fast recycling vesicles (Gaffield and Betz, 2006). For more stringency, we used HBSS buffer without Ca^{2+} or Mg^{2+}, and FM4-64 (0.1 µg/ml) if not mentioned otherwise. Cells grown on a glass coverslip were taken in a chamber with HBSS buffer (1 ml). Dead cells and cellular debris were generally excluded from the view field as these give strong background due to the lipophilic nature of the dye. Dye dissolved in HBSS buffer (50 µl) was added to the cell chamber manually.

F11 cells expressing TRPV1-GFP were treated for dye-loading and/or -unloading experiments. Cells were activated by NADA (0.2 µM) to the cell chamber during the time-series imaging. In other experiments, PMA (1 µM) was added after 1-2 minutes of FM4-64 application. The unloading experiments were done in HBSS bath containing FM4-64 dye.

Measurement of FM4-64 uptake

Cells expressing either TRPV1-GFP or only GFP, or remaining non-transfected, were subjected to FM4-64 incorporation. The cells (in a six-well plate) were washed with 1 ml HBSS buffer (Ca^{2+}-free) and were incubated with the same buffer containing NADA (1 µM, 3 minutes), cytochalasin D (1 µM, 30 minutes) and PMA (1 µM, 3 minutes) before adding FM4-64. In some treatments, cells were treated with ice-cold HBSS buffer for 20 minutes before adding FM4-64. Finally, FM4-64 was added at a final concentration of 0.05 µg/ml. Cells were allowed to label with the dye for only 2 minutes. Cells were metabolically fixed by adding NaN_3 (final concentration 0.2% w/v). All cells were collected by trypsination and further addition of FCS (final concentration 5%) blocked the trypsin effect. The total cell suspension was centrifuged at 1000 ***g*** for 2 minutes. The cell pellet was gently resuspended in 100 µl of HBSS buffer and measured by FACS for their FM4-64 dye content. Origin 6 software was used for all quantification and statistical analysis (independent Student's *t*-test, two populations, significance level 0.05).

Quantification of the spine length

Images of cortical neurons immunostained for TRPV1 and actin were captured by confocal microscopy. 3D images were reconstructed from the *z*-section images. Each spine was marked manually by using the LSM software (Zeiss, Germany). The spines that were too small or ambiguous were not considered. The amount of FM4-64 uptake is represented in arbitrary units. Graphs and statistical information were obtained using Microsoft XL and GraphPad Prism 4 softwares.

We thank Ferdinand Hucho and Christine Andres for their useful inputs. We thank David Bredt, Michael E. Dailey, Shigeo Okabe, Bonnie L. Firestein, Anna Fejtova, Thomas Dresbach and Timothy A. Ryan for their generous help with reagents. Funding from the Max-Planck Institute for Molecular Genetics (Berlin, Germany) is gratefully acknowledged. Further support was granted from the DFG (SFB 779/B9) to E.D.G. C.G. is currently supported by NISER.

Supplementary material available online at
http://jcs.biologists.org/cgi/content/full/123/12/2045/DC1

References

Aguiar, D. C., Terzian, A. L., Guimarães, F. S. and Moreira, F. A. (2009). Anxiolytic-like effects induced by blockade of transient receptor potential vanilloid type 1 (TRPV1) channels in the medial prefrontal cortex of rats. *Psychopharmacology (Berl.)* **205**, 217-225.

Ahmari, S. E., Buchanan, J. and Smith, S. J. (2000). Assembly of presynaptic active zones from cytoplasmic transport packets. *Nat. Neurosci.* **3**, 445-451.

Alter, B. J. and Gereau, R. W., 4th (2008). Hotheaded: TRPV1 as mediator of hippocampal synaptic plasticity. *Neuron* **57**, 629-631.

Atwood, H. L. (2006). Neuroscience. Gatekeeper at the synapse. *Science* **312**, 1008-1009.

Banting, G., Maile, R. and Roquemore, E. P. (1998). The steady state distribution of humTGN46 is not significantly altered in cells defective in clathrin-mediated endocytosis. *J. Cell Sci.* **111**, 3451-3458.

Berghuis, P., Rajnicek, A. M., Morozov, Y. M., Ross, R. A., Mulder, J., Urbán, G. M., Monory, K., Marsicano, G., Matteoli, M., Canty, A. et al. (2007). Hardwiring the brain: endocannabinoids shape neuronal connectivity. *Science* **316**, 1212-1216.

Bernardini, N., Neuhuber, W., Reeh, P. W. and Sauer, S. K. (2004). Morphological evidence for functional capsaicin receptor expression and calcitonin gene-related peptide exocytosis in isolated peripheral nerve axons of the mouse. *Neuroscience* **126**, 585-590.

Bisogno, T., Melck, D., Bobrov M. Y., Gretskaya, N. M., Bezuglov, V. V., De Petrocellis, L. and Di Marzo, V. (2000). N-acyl-dopamines: novel synthetic CB(1) cannabinoid-receptor ligands and inhibitors of anandamide inactivation with cannabimimetic activity in vitro and in vivo. *Biochem. J.* **351**, 817-824.

Blanpied, T. A., Scott, D. B. and Ehlers, M. D. (2002). Dynamics and regulation of clathrin coats at specialized endocytic zones of dendrites and spines. *Neuron* **36**, 435-449.

Boeckers, T. M., Winter, C., Smalla, K. H., Kreutz, M. R., Bockmann, J., Seidenbecher, C., Garner, C. C. and Gundelfinger, E. D. (1999). Proline-rich synapse-associated proteins ProSAP1 and ProSAP2 interact with synaptic proteins of the SAPAP/GKAP family. *Biochem. Biophys. Res. Commun.* **1264**, 247-252.

Bonanomi, D., Fornasiero, E. F., Valdez, G., Halegoua, S., Benfenati, F., Menegon, A. and Valtorta, F. (2008). Identification of a developmentally regulated pathway of membrane retrieval in neuronal growth cones. *J. Cell Sci.* **121**, 3757-3769.

Brauchi, S., Krapivinsky, G., Krapivinsky, L. and Clapham, D. E. (2008). TRPM7 facilitates cholinergic vesicle fusion with the plasma membrane. *Proc. Natl. Acad. Sci. USA* **105**, 8304-8308.

Brewer, G. J., Torricelli, J. R., Evege, E. K. and Price, P. J. (1993). Optimized survival of hippocampal neurons in B27-supplemented Neurobasal, a new serum-free medium combination. *J. Neurosci. Res.* **35**, 567-576.

Caterina, M. J., Schumacher, M. A., Tominaga, M., Rosen, T. A., Levine, J. D. and Julius, D. (1997). The capsaicin receptor: a heat-activated ion channel in the pain pathway. *Nature* **389**, 816-824.

Chen, M., Lucas, K. G., Akum, B. F., Balasingam, G., Stawicki, T. M., Provost, J. M., Riefler, G. M., Jörnsten, R. J. and Firestein, B. L. (2005). A novel role for snapin in dendrite patterning: interaction with cypin. *Mol. Biol. Cell*. **16**, 5103-5114.

Craig, A. M., Graf, E. R. and Linhoff, M. W. (2006). How to build a central synapse: clues from cell culture. *Trends Neurosci*. **29**, 8-20.

Cristino, L., de Petrocellis, L., Pryce, G., Baker, D., Guglielmotti, V. and Di Marzo, V. (2006). Immunohistochemical localization of cannabinoid type 1 and vanilloid transient receptor potential vanilloid type 1 receptors in the mouse brain. *Neuroscience* **139**, 1405-1415.

Cristino, L., Starowicz, K., De Petrocellis, L., Morishita, J., Ueda, N., Guglielmotti, V. and Di Marzo, V. (2008). Immunohistochemical localization of anabolic and catabolic enzymes for anandamide and other putative endovanilloids in the hippocampus and cerebellar cortex of the mouse brain. *Neuroscience* **151**, 955-968.

Cui, M., Honore, P., Zhong, C., Gauvin, D., Mikusa, J., Hernandez, G., Chandran, P., Gomtsyan, A., Brown, B., Bayburt, E. K. et al. (2006). TRPV1 receptors in the CNS play a key role in broad-spectrum analgesia of TRPV1 antagonists. *J. Neurosci*. **26**, 9385-9393.

Di Marzo, V. (2008). Targeting the endocannabinoid system: to enhance or reduce? *Nat. Rev. Drug Discov*. **7**, 438-455.

Di Marzo, V., Gobbi, G. and Szallasi, A. (2008). Brain TRPV1: a depressing TR(i)P down memory lane? *Trends Pharmacol. Sci*. **29**, 594-600.

Doyle, M. W., Bailey, T. W., Jin, Y. H. and Andresen, M. C. (2002). Vanilloid receptors presynaptically modulate cranial visceral afferent synaptic transmission in nucleus tractus solitarius. *J. Neurosci.* **22**, 8222-8229.

Dresbach, T., Torres, V., Wittenmayer, N., Altrock, W. A., Zamorano, P., Zuschratter, W., Nawrotzki, R., Ziv, N. E., Garner, C. C. and Gundelfinger, E. D. (2006). Assembly of active zone precursor vesicles: obligatory trafficking of presynaptic cytomatrix proteins bassoon and piccolo via a *trans*-golgi compartment. *J. Biol. Chem.* **281**, 6038-6047.

Funakoshi, K., Nakano, M., Atobe, Y., Goris, R. C., Kadota, T. and Yazama, F. (2006). Differential development of TRPV1-expressing sensory nerves in peripheral organs. *Cell Tissue Res.* **323**, 27-41.

Gaffield, M. A. and Betz, W. J. (2006). Imaging synaptic vesicle exocytosis and endocytosis with FM dyes. *Nat. Protoc*. **1**, 2916-2921.

Gibson, H. E., Edwards, J. G., Page, R. S., Van Hook, M. J. and Kauer, J. A. (2008). TRPV1 channels mediate long-term depression at synapses on hippocampal interneurons. *Neuron* **57**, 746-759.

Girao, H., Geli, M. I. and Idrissi, F. Z. (2008). Actin in the endocytic pathway: from yeast to mammals. *FEBS Lett.* **582**, 2112-2119.

Goel, M., Sinkins, W. G. and Schilling, W. P. (2002). Selective association of TRPC channel subunits in rat brain synaptosomes. *J. Biol. Chem*. **277**, 48303-48310.

Gomez, T. (2005). Neurobiology: channels for pathfinding. *Nature* **434**, 835-838.

Goswami, C. and Hucho, T. (2007). TRPV1 expression-dependent initiation and regulation of filopodia. *J. Neurochem*. **103**, 1319-1333.

Goswami, C. and Hucho, T. (2008). Submembraneous microtubule cytoskeleton: biochemical and functional interplay of TRP channels with the cytoskeleton. *FEBS J.* **275**, 4684-4699.

Goswami, C., Dreger, M., Jahnel, R., Bogen, O., Gillen, C. and Hucho, F. (2004). Identification and characterization of a Ca^{2+}-sensitive interaction of the vanilloid receptor TRPV1 with tubulin. *J. Neurochem*. **91**, 1092-1103.

Goswami, C., Dreger, M., Otto, H., Schwappach, B. and Hucho, F. (2006). Rapid disassembly of dynamic microtubules upon activation of the capsaicin receptor TRPV1. *J. Neurochem*. **96**, 254-266.

Goswami, C., Hucho, T. B. and Hucho, F. (2007a). Identification and characterisation of novel tubulin-binding motifs located within the C-terminus of TRPV1. *J. Neurochem*. **101**, 250-262.

Goswami, C., Schmidt, H. and Hucho, F. (2007b). TRPV1 at nerve endings regulates growth cone morphology and movement through cytoskeleton reorganization. *FEBS J.* **274**, 760-772.

Greka, A., Navarro, B., Oancea, E., Duggan, A. and Clapham, D. E. (2003). TRPC5 is a regulator of hippocampal neurite length and growth cone morphology *Nat. Neurosci.* **6**, 37-45.

Gundelfinger, E. D., Kessels, M. M. and Qualmann, B. (2003). Temporal and spatial coordination of exo- and endocytosis. *Nat. Rev. Mol. Cell Biol*. **4**, 127-139.

Hjerling-Leffler, J., Alqatari, M., Ernfors, P. and Koltzenburg, M. (2007). Emergence of functional sensory subtypes as defined by transient receptor potential channel expression. *J. Neurosci*. **27**, 2435-2443.

Huang, S. M., Bisogno, T., Trevisani, M., Al-Hayani, A., De Petrocellis, L., Fezza, F., Tognetto, M., Petros, T. J., Krey, J. F., Chu, C. J. et al. (2002). An endogenous capsaicin-like substance with high potency at recombinant and native vanilloid VR1 receptors. *Proc. Natl. Acad. Sci. USA*. **99**, 8400-8405.

Jin, K., Xie, L., Kim, S. H., Parmentier-Batteur, S., Sun, Y., Mao, X. O., Childs, J. and Greenberg, D. A. (2004). Defective adult neurogenesis in CB1 cannabinoid receptor knockout mice. *Mol. Pharmacol*. **66**, 204-208.

Karlsson, U., Sundgren-Andersson, A. K., Johansson, S. and Krupp, J. J. (2005). Capsaicin augments synaptic transmission in the rat medial preoptic nucleus. *Brain Res*. **1043**, 1-11.

Kauer, J. A. and Gibson, H. E. (2009). Hot flash: TRPV channels in the brain. *Trends Neurosci.* **32**, 215-224.

Kittel, R. J., Wichmann, C., Rasse, T. M., Fouquet, W., Schmidt, M., Schmid, A., Wagh, D. A., Pawlu, C., Kellner, R. R., Willig, K. I. et al. (2006). Bruchpilot promotes active zone assembly, Ca^{2+} channel clustering, and vesicle release. *Science* **312**, 1051-1054.

Köfalvi, A., Pereira, M. F., Rebola, N., Rodrigues, R. J., Oliveira, C. R. and Cunha, R. A. (2007). Anandamide and NADA bi-directionally modulate presynaptic Ca^{2+} levels and transmitter release in the hippocampus. *Br. J. Pharmacol*. **151**, 551-563.

Lambers, T. T., Oancea, E., de Groot, T., Topala, C. N., Hoenderop, J. G. and Bindels, R. J. (2007). Extracellular pH dynamically controls cell surface delivery of functional TRPV5 channels. *Mol. Cell. Biol*. **27**, 1486-1494.

Lewinter, R. D., Skinner, K., Julius, D. and Basbaum, A. I. (2004). Immunoreactive TRPV-2 (VRL-1), a capsaicin receptor homolog, in the spinal cord of the rat. *J. Comp. Neurol*. **470**, 400-408.

Li, D., Ropert, N., Koulakoff, A., Giaume, C. and Oheim, M. (2008). Lysosomes are the major vesicular compartment undergoing Ca^{2+}-regulated exocytosis from cortical astrocytes. *J. Neurosci*. **28**, 7648-7658.

Li, H. B., Mao, R. R., Zhang, J. C., Yang, Y., Cao, J. and Xu, L. (2008). Antistress effect of TRPV1 channel on synaptic plasticity and spatial memory. *Biol. Psychiatry* **64**, 286-292.

Li, X. and Eisenach, J. C. (2001). alpha2A-adrenoceptor stimulation reduces capsaicin-induced glutamate release from spinal cord synaptosomes. *J. Pharmacol. Exp. Ther.* **299**, 939-944.

Li, Y., Jia, Y. C., Cui, K., Li, N., Zheng, Z. Y., Wang, Y. Z. and Yuan, X. B. (2005). Essential role of TRPC channels in the guidance of nerve growth cones by brain-derived neurotrophic factor. *Nature* **434**, 894-898.

Maione, S., Cristino, L., Migliozzi, A. L., Georgiou, A. L., Starowicz, K., Salt, T. E. and Di Marzo, V. (2009).TRPV1 channels control synaptic plasticity in the developing superior colliculus. *J. Physiol*. **587**, 2521-2535.

Mandadi, S., Tominaga, T., Numazaki, M., Murayama, N., Saito, N., Armati, P. J., Roufogalis, B. D. and Tominaga, M. (2006). Increased sensitivity of desensitized TRPV1 by PMA occurs through PKCepsilon-mediated phosphorylation at S800. *Pain* **123**, 106-116.

Marinelli, P. W., Funk, D., Juzytsch, W., Harding, S., Rice, K. C., Shaham, Y. and Lê, A. D. (2007). The CRF1 receptor antagonist antalarmin attenuates yohimbine-induced increases in operant alcohol self-administration and reinstatement of alcohol seeking in rats. *Psychopharmacology (Berl.)* **195**, 345-355.

Marinelli, S., Pacioni, S., Bisogno, T., Di Marzo, V., Prince, D. A., Huguenard, J. R. and Bacci, A. (2008). The endocannabinoid 2-arachidonoylglycerol is responsible for the slow self-inhibition in neocortical interneurons. *J. Neurosci*. **28**, 13532-13541.

Marrs, G. S., Green, S. H. and Dailey, M. E. (2001). Rapid formation and remodelling of postsynaptic densities in developing dendrites. *Nat. Neurosci.* **4**, 1006-1013.

Marsch, R., Foeller, E., Rammes, G., Bunck, M., Kössl, M., Holsboer, F., Zieglgänsberger, W., Landgraf, R., Lutz, B. and Wotjak, C. T. (2007). Reduced anxiety, conditioned fear, and hippocampal long-term potentiation in transient receptor potential vanilloid type 1 receptor-deficient mice. *J. Neurosci*. **27**, 832-839.

Matus, A. (2001). Moving molecules make synapses. *Nat. Neurosci.* **4**, 967-968.

Medvedeva, Y. V., Kim, M. S. and Usachev, Y. M. (2008). Mechanisms of prolonged presynaptic Ca^{2+} signaling and glutamate release induced by TRPV1 activation in rat sensory neurons. *J. Neurosci*. **28**, 5295-5311.

Micale, V., Cristino, L., Tamburella, A., Petrosino, S., Leggio, G. M., Drago, F. and Di Marzo, V. (2009). Anxiolytic effects in mice of a dual blocker of fatty acid amide hydrolase and transient receptor potential vanilloid type-1 channels. *Neuropsychopharmacology* **34**, 593-606.

Montell, C. (2004). Exciting trips for TRPs. *Nat. Cell Biol.* **6**, 690-692.

Morenilla-Palao, C., Planells-Cases, R., Garcia-Sanz, N. and Ferrer-Montiel. (2004). Regulated exocytosis contributes to protein kinase C potentiation of vanilloid receptor activity. *J. Biol. Chem.* **279**, 25665-25672.

Nakata, T., Terada, S. and Hirokawa, N. (1998). Visualization of the dynamics of synaptic vesicle and plasma membrane proteins in living axons. *J. Cell Biol*. **140**, 659-674.

Newey, S. E., Velamoor, V., Govek, E. E. and Van Aelst, L. (2005). Rho GTPases, dendritic structure, and mental retardation. *J. Neurobiol*. **64**, 58-74.

Okabe, S., Kim, H. D., Miwa, A., Kuriu, T. and Okado, H. (1999). Continual remodeling of postsynaptic density and its regulation by synaptic activity. *Nat. Neurosci.* **2**, 804-811.

Okabe, S., Urushido, T., Konno, D., Okado, H. and Sobue, K. (2001). Rapid redistribution of the postsynaptic density protein PSD-Zip45 (Homer 1c) and its differential regulation by NMDA receptors and calcium channels. *J. Neurosci.* **21**, 9561-9571.

Pannese, E. (1994). *Neurocytology: Fine Structure of Neurons, Nerve Processes and Neuroglial Cells*, 264 pp. New York: Thieme Medical Publishers, Inc.

Panzer, J. A., Song, Y. and Balice-Gordon, R. J. (2006). In vivo imaging of preferential motor axon outgrowth to and synaptogenesis at prepatterned acetylcholine receptor clusters in embryonic zebrafish skeletal muscle. *J. Neurosci*. **26**, 934-947.

Platika, D., Boulos, M. H., Baizer, L. and Fishman, M. C. (1985). Neuronal traits of clonal cell lines derived by fusion of dorsal root ganglia neurons with neuroblastoma cells. *Proc. Natl. Acad. Sci. USA* **82**, 3499-3503.

Qin, L., Marrs, G. S., McKim, R. and Dailey, M. E. (2001). Hippocampal mossy fibers induce assembly and clustering of PSD95-containing postsynaptic densities independent of glutamate receptor activation. *J. Comp. Neurol*. **440**, 284-298.

Rácz, B., Blanpied, T. A., Ehlers, M. D. and Weinberg, R. J. (2004). Lateral organization of endocytic machinery in dendritic spines. *Nat. Neurosci*. **7**, 917-918.

Rhee, J. S., Betz, A., Pyott, S., Reim, K., Varoqueaux, F., Augustin, I., Hesse, D., Sudhof, T. C., Takahashi, M., Rosenmund, C. et al. (2002). Beta phorbol ester- and diacylglycerol-induced augmentation of transmitter release is mediated by Munc13s and not by PKCs. *Cell* **108**, 121-133.

Rimmerman, N., Bradshaw, H. B., Basnet, A., Tan, B., Widlanski, T. S. and Walker, J. M. (2009). Microsomal omega-hydroxylated metabolites of N-arachidonoyl dopamine are active at recombinant human TRPV1 receptors. *Prostaglandins Other Lipid Mediat*. **88**, 10-17.

Roberts, J. C., Davis, J. B and Benham, C. D. (2004). [^{3}H]Resiniferatoxin autoradiography in the CNS of wild-type and TRPV1 null mice defines TRPV1 (VR-1) protein distribution. *Brain Res*. **995**, 176-183.

Roos, J. and Kelly, R. B. (2000). Preassembly and transport of nerve terminals: a new concept of axonal transport. *Nat. Neurosci.* **3**, 415-417.

Sabo, S. L. and McAllister, A. K. (2003). Mobility and cycling of synaptic protein-containing vesicles in axonal growth cone filopodia. *Nat. Neurosci.* **6**, 1264-1269.

Sabo, S. L., Gomes, R. A. and McAllister, A. K. (2006). Formation of presynaptic terminals at predefined sites along axons. *J. Neurosci*. **26**, 10813-10825.

Sagar, D. R., Smith, P. A., Millns, P. J., Smart, D., Kendall D. A. and Chapman, V. (2004). TRPV1 and CB(1) receptor mediated effects of the endovanilloid/endocannabinoid N arachidonoyl dopamine on primary afferent fibre and spinal cord neuronal responses in the rat. *Eur. J. Neurosci.* **20**, 175-184.

Schicho, R., Donnerer, J., Liebmann, I. and Lippe, I. T. (2005). Nociceptive transmitter release in the dorsal spinal cord by capsaicin-sensitive fibers after noxious gastric stimulation. *Brain Res*. **1039**, 108-115.

Schmid, G., Carita, F., Bonanno, G. and Raiteri, M. (1998). NK-3 receptors mediate enhancement of substance P release from capsaicin-sensitive spinal cord afferent terminals. *Br. J. Pharmacol.* **125**, 621-626.

Shibasaki, K., Suzuki, M., Mizuno, A. and Tominaga, M. (2007). Effects of body temperature on neural activity in the hippocampus: regulation of resting membrane potentials by transient receptor potential vanilloid 4. *J. Neurosci.* **27**, 1566-1575.

Shim, S., Goh, E. L., Ge, S., Sailor, K., Yuan, J. P., Roderick, H. L., Bootman, M. D., Worley, P. F., Song, H. and Ming, G. L. (2005). XTRPC1-dependent chemotropic guidance of neuronal growth cones. *Nat. Neurosci.* **8**, 730-735.

Sikand, P. and Premkumar, L. S. (2007). Potentiation of glutamatergic synaptic transmission by protein kinase C-mediated sensitization of TRPV1 at the first sensory synapse. *J. Physiol*. **581**, 631-647.

Singh, B. B., Lockwich, T. P., Bandyopadhyay, B. C., Liu, X., Bollimuntha, S., Brazer, S. C., Combs, C., Das, S., Leenders, A. G., Sheng, Z. H. et al. (2004). VAMP2-dependent exocytosis regulates plasma membrane insertion of TRPC3 channels and contributes to agonist-stimulated Ca^{2+} influx. *Mol. Cell*. **15**, 635-646.

Starowicz, K., Maione, S., Cristino, L., Palazzo, E., Marabese, I., Rossi, F., de Novellis, V. and Di Marzo, V. (2007a). Tonic endovanilloid facilitation of glutamate release in brainstem descending antinociceptive pathways. *J. Neurosci*. **27**, 13739-13749.

Starowicz, K., Nigam, S. and Di Marzo, V. (2007b). Biochemistry and pharmacology of endovanilloids. *Pharmacol. Ther*. **114**, 13-33.

Starowicz, K., Cristino, L. and Di Marzo, V. (2008). TRPV1 receptors in the central nervous system: potential for previously unforeseen therapeutic applications. *Curr. Pharm. Des*. **14**, 42-54.

Steenland, H. W., Ko, S. W., Wu, L. J. and Zhuo, M. (2006). Hot receptors in the brain. *Mol. Pain* **2**, 34.

Tóth, A., Boczán, J., Kedei, N., Lizanecz, E., Bagi, Z., Papp, Z., Edes, I., Csiba, L. and Blumberg, P. M. (2005). Expression and distribution of vanilloid receptor 1 (TRPV1) in the adult rat brain. *Mol. Brain Res.* **135**, 162-168.

Tóth, A., Blumberg, P. M. and Boczán, J. (2009). Anandamide and the vanilloid receptor (TRPV1). *Vitam. Horm*. **81**, 389-419.

Valtschanoff, J. G., Rustioni, A., Guo, A. and Hwang, S. J. (2001). Vanilloid receptor VR1 is both presynaptic and postsynaptic in the superficial laminae of the rat dorsal horn. *J. Comp. Neurol.* **436**, 225-235.

Verstreken, P., Ohyama, T. and Bellen, H. J. (2008). FM 1-43 labeling of synaptic vesicle pools at the Drosophila neuromuscular junction. *Methods Mol. Biol*. **440**, 349-369.

Vizi, E. S., Kiss, J. P. and Lendvai, B. (2004). Nonsynaptic communication in the central nervous system. *Neurochem. Int*. **45**, 443-451.

Walter, S., Sandig, K., Hinkel, G. K., Mitulla, B., Ounap, K., Sims, G., Sitska, M., Utermann, B., Viertel, P., Kalscheuer, V. et al. (2004). Subtelomere FISH in 50 children with mental retardation and minor anomalies, identified by a checklist, detects 10 rearrangements including a de novo balanced translocation of chromosomes 17p13.3 and 20q13.33. *Am. J. Med. Genet. A* **128**, 364-373.

Wang, G. X. and Poo, M. M. (2005). Requirement of TRPC channels in netrin-1-induced chemotropic turning of nerve growth cones. *Nature* **434**, 898-904.

Wimmer, V. C., Horstmann, H., Groh, A. and Kuner, T. (2006). Donut-like topology of synaptic vesicles with a central cluster of mitochondria wrapped into membrane protrusions: a novel structure-function module of the adult calyx of Held. *J Neurosci.* **26**, 109-116.

Wyneken, U., Smalla, K. H., Marengo, J. J., Soto, D., de la Cerda, A., Tischmeyer, W., Grimm, R., Boeckers, T. M., Wolf, G., Orrego, F. et al. (2001). Kainate-induced seizures alter protein composition and N-methyl-D-aspartate receptor function of rat forebrain postsynaptic densities. *Neuroscience* **102**, 65-74.

Xing, J. and Li, J. (2007). TRPV1 receptor mediates glutamatergic synaptic input to dorsolateral periaqueductal gray (dl-PAG) neurons. *J. Neurophysiol*. **97**, 503-511.

Zhu, P. C., Thureson-Klein, A. and Klein, R. L. (1986). Exocytosis from large-dense cored vesicles outside the active synaptic zones of terminals within the trigeminal subnucleus caudalis: a possible mechanism for neuropeptide release. *Neuroscience* **19**, 43-54.

Zimov, S. and Yazulla, S. (2004). Localization of vanilloid receptor 1 (TRPV1/VR1)-like immunoreactivity in goldfish and zebrafish retinas: restriction to photoreceptor synaptic ribbons. *J. Neurocytol*. **33**, 441-452.

Journal of Cell Science